RSC Advances

PAPER

View Article Online
View Journal | View Issue

Cite this: *RSC Adv.*, 2020, **10**, 30254

Structural characterization of a novel *Lactarius volemus* Fr. polysaccharide and its immunity activity in BALB/c mice

Yan-yan Huang,[a] Jia-jia Yu,[a] Juan Huang,[ab] Dong-mei Liu *[a] and Ming-hua Liang*[a]

Received 12th June 2020
Accepted 24th July 2020

DOI: 10.1039/d0ra05176d

rsc.li/rsc-advances

Lactarius volemus Fr. has been regarded as a great edible medicinal fungal resource in China. In this study, *L. volemus* Fr. polysaccharide (LVP) with an average molecular weight of 16.842 kDa was obtained by water extraction. The structure of LVP was characterized to be mannan, and the linkages in the mannan were found to comprise the Man*p*, (1→4)-α-Man and (1→4,6)-α-Man. Furthermore, intraperitoneal administration of LVP increased the thymus, spleen and liver indices, dose-dependently. Additionally, LVP enhanced the immune response and the phagocytic activities. Pathological evaluations showed that LVP in mice increased the proliferation of red medullary lymphocytes (60–70%). Collectively, these results indicated that LVP might be a potential resource of raw material for further investigations of functional foods.

1. Introduction

China is rich in wild edible fungus resources. Many kinds of edible fungi have been proved to have a broad range of disease resistance, low toxicity and few side effects.[1] Polysaccharides of edible fungi have become research hotspots due to their unique physiological activity.[2–5] *Shiraia bambusicola*, a bamboo symbiotic fungus, contains galactofuranose (Galf), and exhibits immunity activities by activating macrophages.[6] Previous studies revealed that the *Hericium erinaceus* polysaccharide fraction possessed significant immunomodulatory activity by promoting T and B lymphocyte multiplication and IL-2, IL-4, IFN-γ secretion in mice.[2] *Lentinula edodes* was one of the most widely studied mushrooms regarding its immunomodulatory potential. Purified β and α-D-glucans from *Lentinula edodes* reduced the secretion of IL-1β and IL-6 in macrophages.[3] Therefore, edible-medicinal fungi are principal sources of bioactive polysaccharides.

Lactarius volemus Fr., also named milkcap, is a species of ectomycorrhizal fugus in the genus *Lactarius*, family Russulaceae, order Russulales, which is planted in provinces such as Yunnan and Guizhou in China.[7,8] In China, it has been regarded as a significant medical and edible fungi resource, but usually exploited as fried food in daily life and tires used in the rubber industry for its fruiting body can produce high polyisoprene olefins. The main components of *L. volemus* Fr. are polysaccharides, organic acids, phenols, and sesquiterpenes. Kobata has isolated one sterol with a heptanorergostane skeleton and two known sterols from the neutral component of *L. volemus*.[4] The inhibitory rates of *L. volemus* to mouse sarcoma and type A cancer were 80% and 90%, respectively.[9] However, there is still little information on the extraction of bioactive polysaccharides from *L. volemus* Fr., which may impede their production and development for healthcare products, diet programs, and public nutrition.

In the immunosuppressed mouse modeling, animal was usually treated with cyclophosphamide (CP) which has strong cytotoxic and immunosuppressive effects.[10–12] It is well known that non-specific immunity is an important part of the immunity system of the body to prevent the human body from being infected by microorganisms and prevent cancer.[13] Macrophages play a significant role in the immune response process. Activated macrophages can express toll-like receptors (TLRs), selectively recognize pathogen-related molecular patterns, and initiate natural immune responses.[14,15] Although immunostimulation inducing bioactive molecules is a significantly interesting theme to researchers, the immunological activity of polysaccharides from *L. volemus* Fr. is less studied.

Previous studies have demonstrated that *L. volemus* Fr. polysaccharide extracts on three types of probiotic yogurts could prolong the guarantee period of yogurts.[16] However, more studies should concentrate on the identification of structure this new polysaccharide including monosaccharide elements and the classification of glycosidic bonds. Therefore, this study focused on the new polysaccharide named LVP purified from *L. volemus* Fr. The main structure characterizations of LVP were evaluated. Furthermore, its immunity activity was assessed using BALB/c mice with or without LVP at the dose of 200–

[a]*School of Food Science and Engineering, South China University of Technology, Guangzhou 510640, Guangdong, China. E-mail: liudm@scut.edu.cn; liangmh@scut.edu.cn; Fax: +86-20-87113848; Tel: +86-20-222368198; +86-13-609795325; +86-15-017539128*

[b]*Guangdong Yantang Dairy Co., Ltd., Guangzhou 510640, Guangdong, China*

800 mg kg^{-1} bw^{-1}. Our work attempted to provide new and useful information about LVP and a better understanding of the structure and molecular conformation for LVP, which is important for clear clarification of its immunity activities related to the molecular structure.

2. Materials and methods

2.1 Materials and reagents

L. volemus Fr. was accumulated in a pine forest of Chuxiong City in Yunnan province. Grind the air-dried *L. volemus* Fr. with a high-speed disintegrator, then pass through a 200-mesh sieve. Cyclophosphamide (CP) was acquired from Jiangsu Heng Rui Medicine Co., Ltd (Lianyungang, Jiangsu, China). Sheep erythrocytes (SRBC) were purchased from Guangzhou Shuvo Heng Biotechnology Co., Ltd. All other chemicals used were of analytical grade. The ultrapure water was utilized from a Milli-Q water purification system (Millipore, Bedford, MA, USA).

2.2 Extraction and purification of polysaccharide from *L. volemus* Fr.

L. volemus Fr. was accumulated in a pine forest and utilized for polysaccharide extraction in Fig. 1A according to Villares (2013).[17] Two grams of the dried sample after pretreatment were mixed with distilled water at a ratio of 1 : 30, and then the method of water extraction and alcohol precipitation was used to obtain polysaccharide after ultrasonic treatment. The experimental conditions were as follows: the ultrasonic power was 100 W for 10 min, the water bath temperature was 95 °C for 4 h, the volume ratio of water extracts and cold ethanol was 1 : 3, and ethanol precipitation time was 24 h. The sample was then mixed with a quarter of to remove protein, and dialyzed using a dialysis bag (3500 Da) for 24 hours. The sample was freeze-dried to obtain crude polysaccharide (CLVP). The DEAE-52 anion-exchange chromatography (50 cm × 2.6 cm) was used for purification of the CLVP, eluted with gradient concentrations of NaCl solutions (0, 0.05, 0.10, 0.15, 0.20, 0.25, 0.30, 0.35 and 0.4 mol L^{-1}) at the flow rate of 0.4 mL min^{-1}, and each conical flask received 200 mL of eluent. The phenol-sulfuric acid method was used for testing the absorbance of each conical flask at 490 nm to collect nine fractions (CLVP-1–CLVP-9)[18]. The purified CLVP-1 was collected and loaded into a Sephadex G-150 column (1.6 cm × 50 cm), and eluted with 0.9% NaCl at a flow rate of 1.0 mL min^{-1}. Each receiving tube gathered 10 mL of eluent, and the absorbance of each receiving tube was determined at 490 nm using the phenol-sulfuric acid method. The combined peak tube eluate was collected and freeze-dried to gain a homogenous polysaccharide, named as LVP.

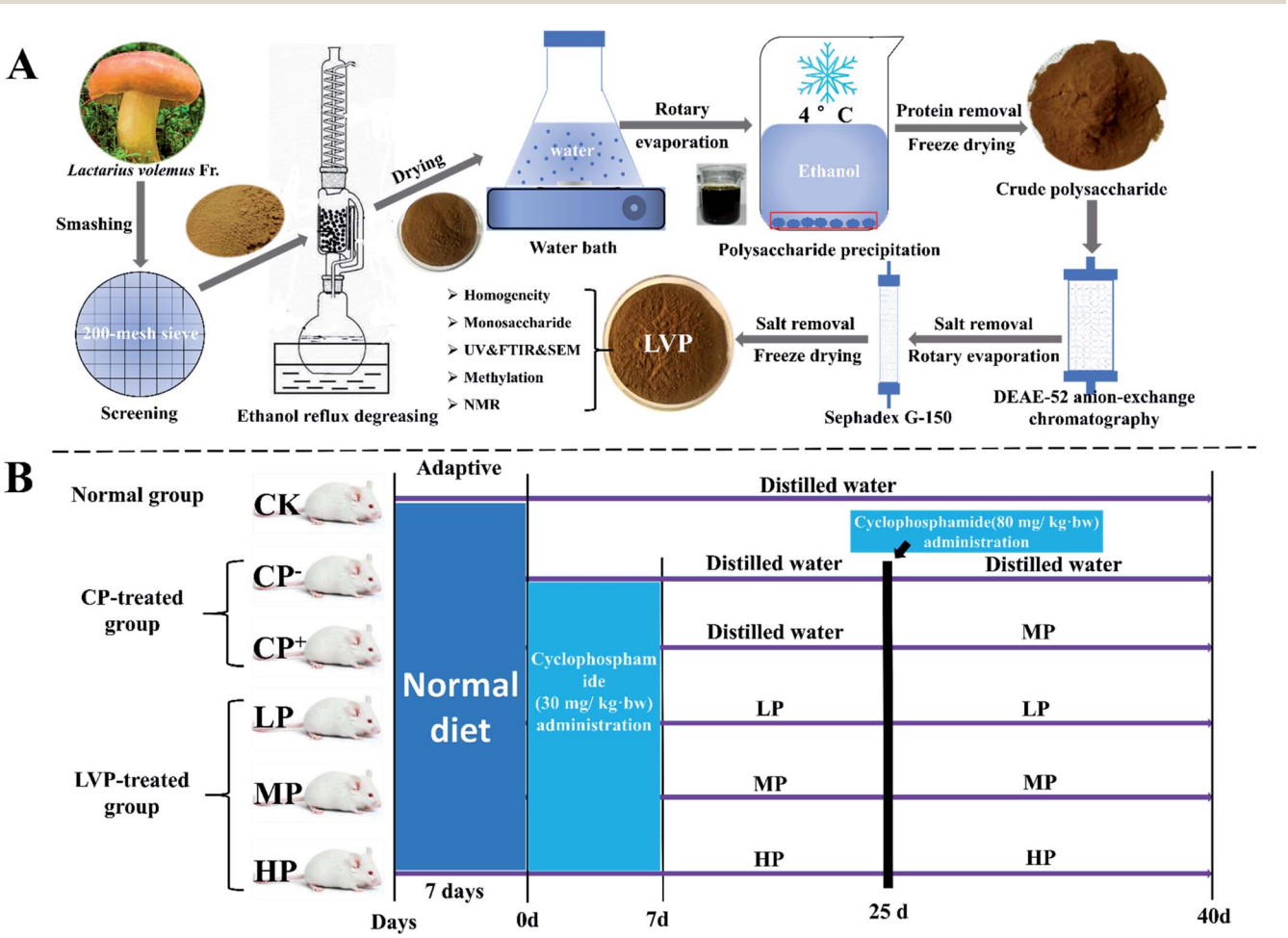

Fig. 1 Schematic diagram for the brief preparation process of LVP (A) and experimental design of BALB/c mice (B).

2.3 General properties analysis of LVP

Homogeneity and weight of the extracted LVP were measured by high performance gel permeation chromatography (HPGPC) with a TSK gel G3000 PWXL column (300 mm × 7.8 mm, Tokyo, Japan). Briefly, LVP (5 mg) was dissolved in 1 mL 0.02 M KH_2PO_4 solution (pH 7.0). 20 μL of the solution was filtered by a 0.45 μm filter, then the sample was injected into a 1525 GPC system (Waters, USA), and the column temperature was 35 °C. The molecular weight was evaluated by reference to the various dextran standards (from 5.0 kDa to 670 kDa).

Monosaccharide composition of LVP from *L. volemus* Fr. was analyzed by the modified HPLC method.[19] Briefly, 10 mg of LVP was hydrolyzed (110 °C, 5 h) with hydrochloric acid (4 M, 10 mL), then was treated by centrifugation (8000 rpm, 10 min). The supernatant was gathered and dried under reduced pressure by adding methanol three times followed by adding 10 mL distilled water. Then, 1-phenyl-3-methyl-5-pyrazolone (PMP) and NaOH (0.3 M) were mixed with the sample at 70 °C for 30 min. Chloroform was added to the mixture for removing excess PMP. Finally, the resulting solution was ready for HPLC analysis after filtering by a 0.45 μm filter. The standard D-mannose was also derivatized under the same condition. The proportion of monosaccharide composition in the sample was calculated from the peak area of each monosaccharide. HPLC detection was carried out at 25 °C using a C18 column (5 μm, 4.6 × 250 mm, Venusil MP-C18, USA) with a HPLC Ultimate 3000 system (Thermo scientific, USA). The mobile phase included solvent A (15% acetonitrile in 0.05 M potassium dihydrogen phosphate buffer, pH 6.9) and solvent B (40% acetonitrile in the same buffer). The gradient pattern was as followed: 0 → 10 → 30 → 35 → 40 min, corresponding to solvent B: 0 → 8 → 20 → 30 → 8% at flow rate of 1 mL min^{-1}.

2.4 Chemical characteristics analysis of LVP

Chemical characteristics of LVP were analyzed by ultraviolet (UV) scanning spectrum, Fourier-Transform Infrared Spectroscopy (FTIR), and scanning electron microscopy (SEM). The UV scanning spectrum was rapidly scanned at an interval of 1 nm to collect the UV absorption spectrum of LVP in the wavelength range of 200–400 nm. For FTIR, the LVP was mixed with KBr powder, ground and pressed into 1 mm pellet for FTIR analysis in the frequency range of 4000–500 cm^{-1} at a resolution of 4 cm^{-1}. The scanning electron microscope (S-3700N, Hitachi, Japan) was used to morphology observation.[20]

2.5 Periodate oxidation and Smith degradation

Fifty mg dried samples were reacted with 50 mL 15 mM $NaIO_4$ under 4 °C in the dark. Ten μL of solution was taken every 4 h and the absorbance was measured at 223 nm until the absorbance was stable, and then ethylene glycol was added to the resulting solution for removing the excessive $NaIO_4$. The formic acid produced by the degradation process was titrated with 0.01 M NaOH and phenolphthalein was used as an indicator. The remaining solution was mixed with 120 mg $NaBH_4$ for 24 h in the dark and then counteracted to pH 5.5 with 0.1 M acetic acid. The trace solution was dialyzed for 48 h at 4 °C and freeze-dried at −50 °C below 10 Pa for 48 h. Then 20 mg lyophilizate was hydrolyzed (120 °C, 3 h) with 2 M trifluoroacetic acid (TFA), and followed by acetylating (90 °C, 30 min) with pyridine (1 mL) and hydroxylamine hydrochloride (10 mg). Another acetic anhydride (1 mL) was added to continue the reaction for 30 min. The acetylated products were dissolved with dichloromethane (1 mL) and filtered by a 0.22 μm organic membrane. The sample was analyzed by using GC-MS (Agilent, USA) with an INNO-WAX capillary column (30 m × 0.25 mm × 0.25 μm). The heating conditions were at 10 °C min^{-1} in the range of 150–180 °C and then at 15 °C min^{-1} in the range of 180–260 °C.

2.6 Methylation analysis of LVP

Dimethyl sulfoxide (DMSO) was used to dissolve 60 mg of LVP (dried), and methyl iodide (CH_3I) was added, then the solution was treated with ultrasound and agitation for 30 min. Afterward, distilled water was added into the solution for removing the remaining methyl iodide. The methylated sample was hydrolyzed and mixed with 10 mg of hydroxylamine hydrochloride, 1 mg of inositol and 1.0 mL of pyridine by the reaction at 90 °C for 30 min. The acetate derivative was analyzed by GC-MS on an HP6890II/5973 instrument with a DB-5 ms fused silica capillary column (30 mm × 0.25 mm × 0.25 μm) (Agilent Technologies, USA). The heating conditions were at 2 °C min^{-1} in the scope of 120–160 °C, and at 3 °C min^{-1} in the scope of 160–250 °C and then kept for 12 min. Both the injector and detector temperatures were 250 °C.

2.7 NMR analysis of LVP

One hundred mg dried LVP was dissolved in 0.6 mL deuterium oxide (D_2O) for two days, then freeze-dried and dissolved in 0.6 mL D_2O again to ensure the H/D exchange completely. The ^1H and ^{13}C spectra of LVP were measured by a Bruker NMR spectrometer (AVANCE III HD 600, Bruker, Germany).

2.8 Immunomodulatory activity analysis of LVP

2.8.1 Animals and experimental design. All animal procedures were performed in accordance with the Guidelines for Care and Use of Laboratory Animals of Sun Yat-sen University (license number: SCXK 2012-0081) and experiments were approved by the Animal Ethics Committee of Guangdong Medical Laboratory Animal Center (animal use permit: SCXK 2013-0002). SPF BALB/c mice (male), with an average weight of 20 ± 2 g, were bought from Guangdong Provincial Medical Laboratory Animal Center. All mice were adapted to the experimental environment for one week (22 ± 1 °C, 45–55% humidity, and normal day/night cycle). After being adapted to the facility surroundings for one week, the mice were arranged into six groups at random (12 mice for each group) in Fig. 1B. Except the control group (CK), other experimental groups were squirted intraperitoneally with cyclophosphamide (CP) at day 1 to day 7 (30 mg kg^{-1} bw^{-1} CP) and day 25 (80 mg kg^{-1} bw^{-1} CP) to establish immunosuppressed models. CP-treated immunosuppressed mice were intraperitoneal administrated daily: negative model group (CP^-) and positive model group (CP^+) with distilled water, while CP^+ group with LVP

at 400 mg kg^{-1} bw^{-1} after day 25. LVP-treated groups (LP, MP, and HP) were treated with LVP at the dose of 200, 400 and 800 mg kg^{-1} bw^{-1} at day 7 to day 40, respectively. The normal group was treated with distilled water. The animals were fed for a 40 day period. The body weight was measured weekly, and the food intake was measured daily.

2.8.2 Effects of LVP on immune organs in immunosuppressed mice. About 24 h after the last feeding, the thymus, spleen, and liver of the mice were weighed for calculating the thymus, spleen, and liver indices, and the calculation method was as follows:[27]

$$\text{Thymus, spleen or liver index} = (\text{weight of thymus, spleen or liver/body weight}) \times 100 \quad (1)$$

2.8.3 Effect of LVP on delayed hypersensitivity (DTH) in immunosuppressed mice. Animals were inoculated intradermally with 2% sheep red blood cells (SRBCs) suspensions (0.2 mL) for 24 h on the right foot of each mouse for the test after the last administration. Delayed-type hypersensitivity (DTH) responses were expressed as the difference between the plantar part thickness at the time of inoculation and that 96 h later.

$$\text{The DTH rate} = \frac{T_1 - T_0}{T_0} \times 100 \quad (2)$$

where T_1 and T_0 are the thickness of right and left foot, respectively.

2.8.4 Effect of LVP on mononuclear phagocytic system (MPS) function by carbon clearance test in immunosuppressed mice. Mice were fasted overnight after the last feeding. The Indian ink was diluted 3–4 times with physiological saline (0.1 mL/10 g), and then injected into mice from the tail vein. At 2 min (t_1) and 12 min (t_2), blood (20 μL) was obtained from the retroorbital venous plexus of each mouse and admixed immediately with 2 mL of 0.1% sodium carbonate. The 0.1% sodium carbonate (2 mL) was mixed with the blood obtained of from the retroorbital venous plexus of the mice at 2 min (t_1) and 12 min (t_2), respectively. Optical density (OD) at 600 nm was determined (OD_1 for t_1 and OD_2 for t_2) with the 0.1% sodium carbonate used as a control. The mice were executed after weighing. The liver and spleen of each mouse were removed. The floating blood was washed with 0.9% physiological saline, and water was absorbed with the filter paper. Each liver and spleen were weighed separately. The phagocytic index was calculated as follows:[24]

$$\text{Carbon clearance index } K = \frac{\lg OD_1 - \lg OD_2}{t_2 - t_1} \quad (3)$$

$$\text{Phagocytic index } \alpha = \frac{A}{B + C} \times \sqrt[3]{K} \quad (4)$$

where A is the body weight, B is the liver weight and C is the spleen weight.

2.8.5 Effect of LVP on serum half hemolysis levels (HC_{50}) in immunosuppressed mice. The production of hemolysis immunized with sheep red blood cells (SRBC) was determined as the Lodmell's method.[25] Briefly, the mouse was injected 0.2 mL SRBC suspension (10^9 mL^{-1}) for immunity test. Since the last administration, 1.5 h later, the blood samples were gathered. One hour later, these blood samples were treated by centrifugation (2000 rpm, 10 min). 5 μL serum was mixed with 995 μL SA buffer (pH = 7.4) (NA-Vander Biotech) to obtain diluted serum (multiple of serum dilution = 200). 1 mL of the supernatant was mixed with 3 mL of Drabkin's solution. Ten minutes later, the absorbance (OD) was measured at 540 nm.

$$HC_{50} = \text{multiple of serum dilution} \times OD_{\text{the sample}}/OD_{\text{control}} \quad (\text{multiple of serum dilution} = 200) \quad (5)$$

2.8.6 Effect of LVP on lymphocytes proliferation in immunosuppressed mice. In the final stage of the experiment, the mice were fasted for one night. The mouse eyeballs were removed, and the whole mouse blood was collected in the EDTA anticoagulant tubes and placed in an icebox. The white blood cells (WBC), the number of lymphocyte immune cells (LYM), and the proportion of lymphocyte to whole blood cells (LYM%) in whole blood of mice in each group were determined by Autoanalyzer (HITACHI 7180, Japan) analysis.

2.8.7 Gross observation and pathological sections of liver, spleen and thymus tissues. The mice were sacrificed on the forty-first day, the liver, spleen and thymus were removed, and the overall morphology and surface color were recorded and photographed. After weighing, the left lobe of the liver was dehydrated, embedded in paraffin, sliced, and hematoxylin–eosin stained,[26] and then observed with a LEICA DM5000B optical microscope (Leica Instrument, Germany).

2.9 Statistical analysis

The experimental data was analyzed by Origin Pro 8.0 software (Stat-Ease Inc., Minneapolis, USA). Results were expressed as the mean ± SD. A one-way ANOVA followed by Tukey's HSD test was used for multiple comparisons with SPSS 19.0 (SPSS, Inc, Chicago, IL, USA). $p < 0.05$ was considered to indicate a significant difference.

3. Results and discussion

3.1 Extraction and purification of polysaccharides from *L. volemus* Fr.

CLVPs (36 g) were isolated from 200 g dried *L. volemus* Fr. by water extraction and ethanol precipitation, and the extraction rate was 18%. The dried LVP (1.041 g) was obtained with a yield of 0.52% from CLVP after separation through DEAE-52 anion-exchange chromatography (Fig. 2A) and Sephadex G-150 (Fig. 2B). Owing to the good biological activities of neutral water-soluble polysaccharides, we mainly concentrated on LVP (eluted by distilled water).

3.2 Molecular weight and monosaccharide composition of LVP

The purity and molecular weight of LVP were analyzed by HPGPC. A single peak of LVP was observed (Fig. 2C) showing that LVP was

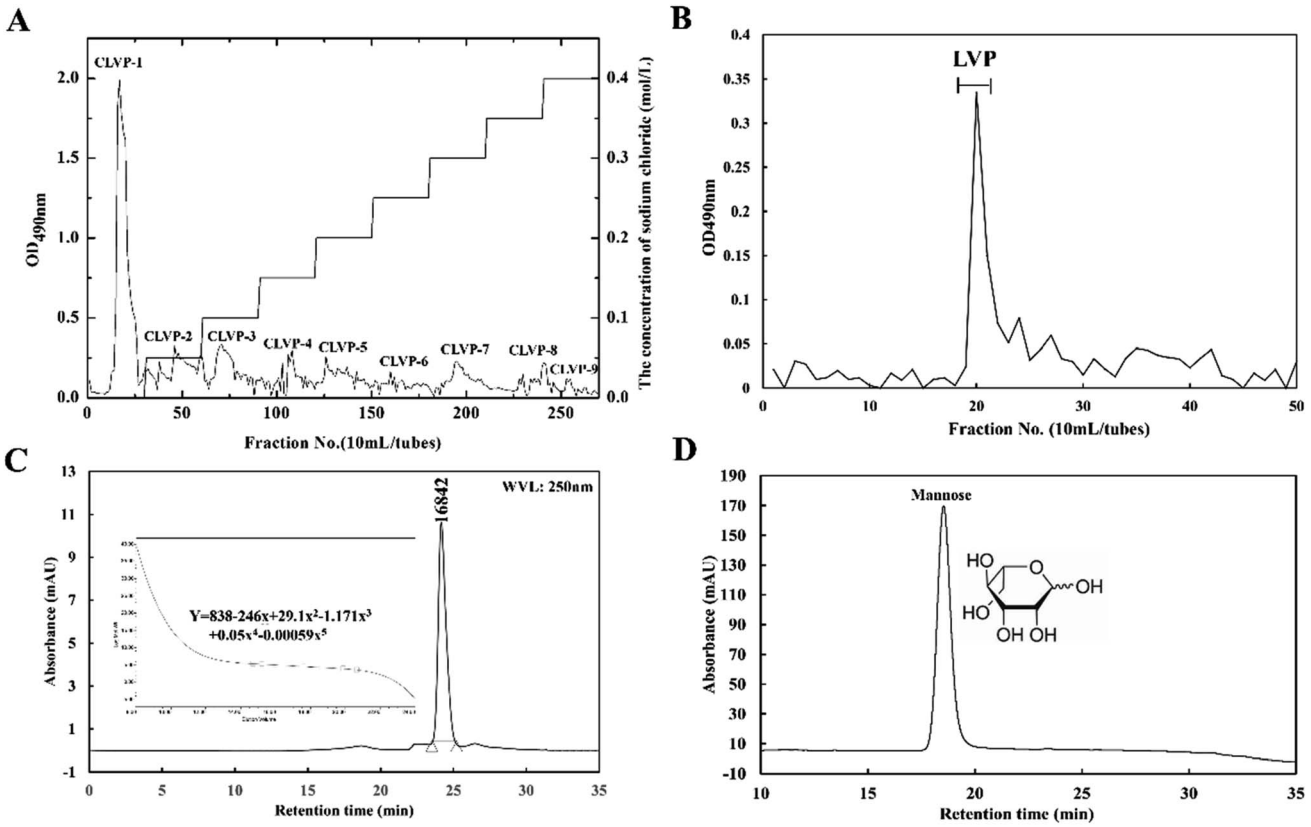

Fig. 2 Chromatograms of LVP from *L. volemus* Fr. purified by (A) DEAE-52 anion-exchange chromatography, (B) Sephadex G-150 column, and (C) HPGPC. (D) HPLC analysis of monosaccharide composition of LVP.

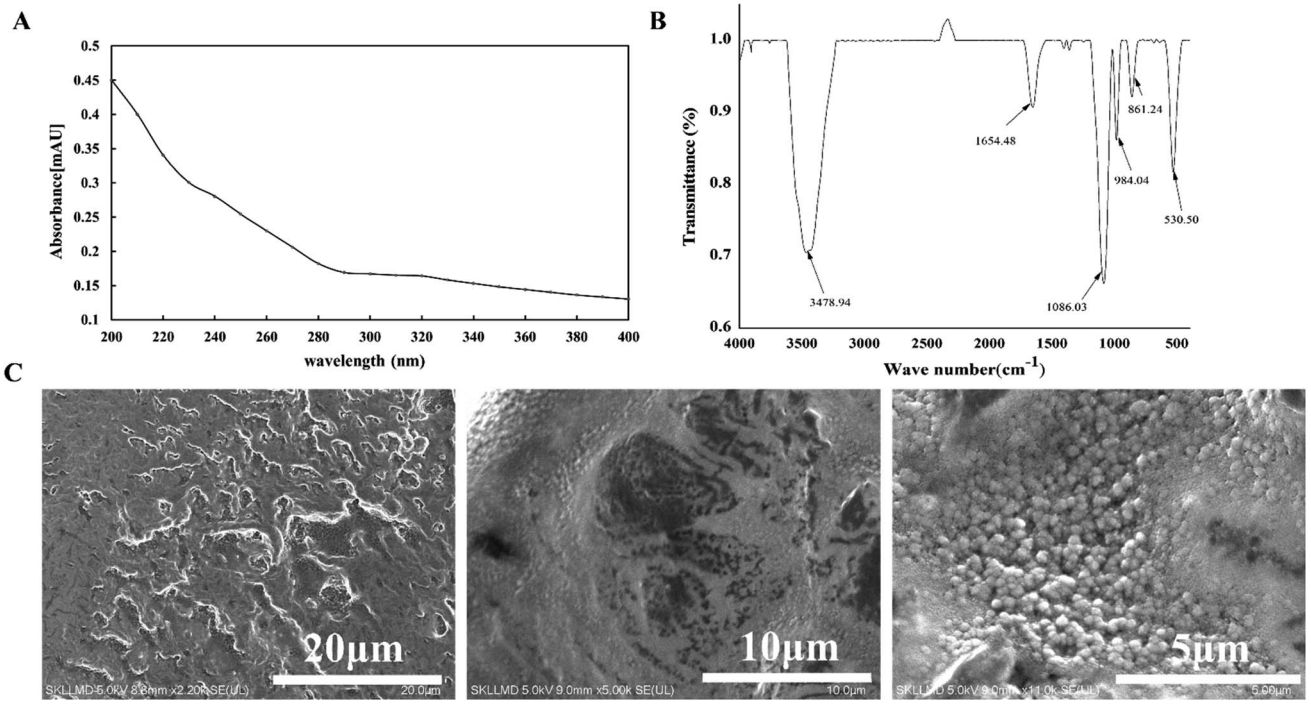

Fig. 3 UV (A), FTIR (B) and SEM images (C) of LVP from *L. volemus* Fr.

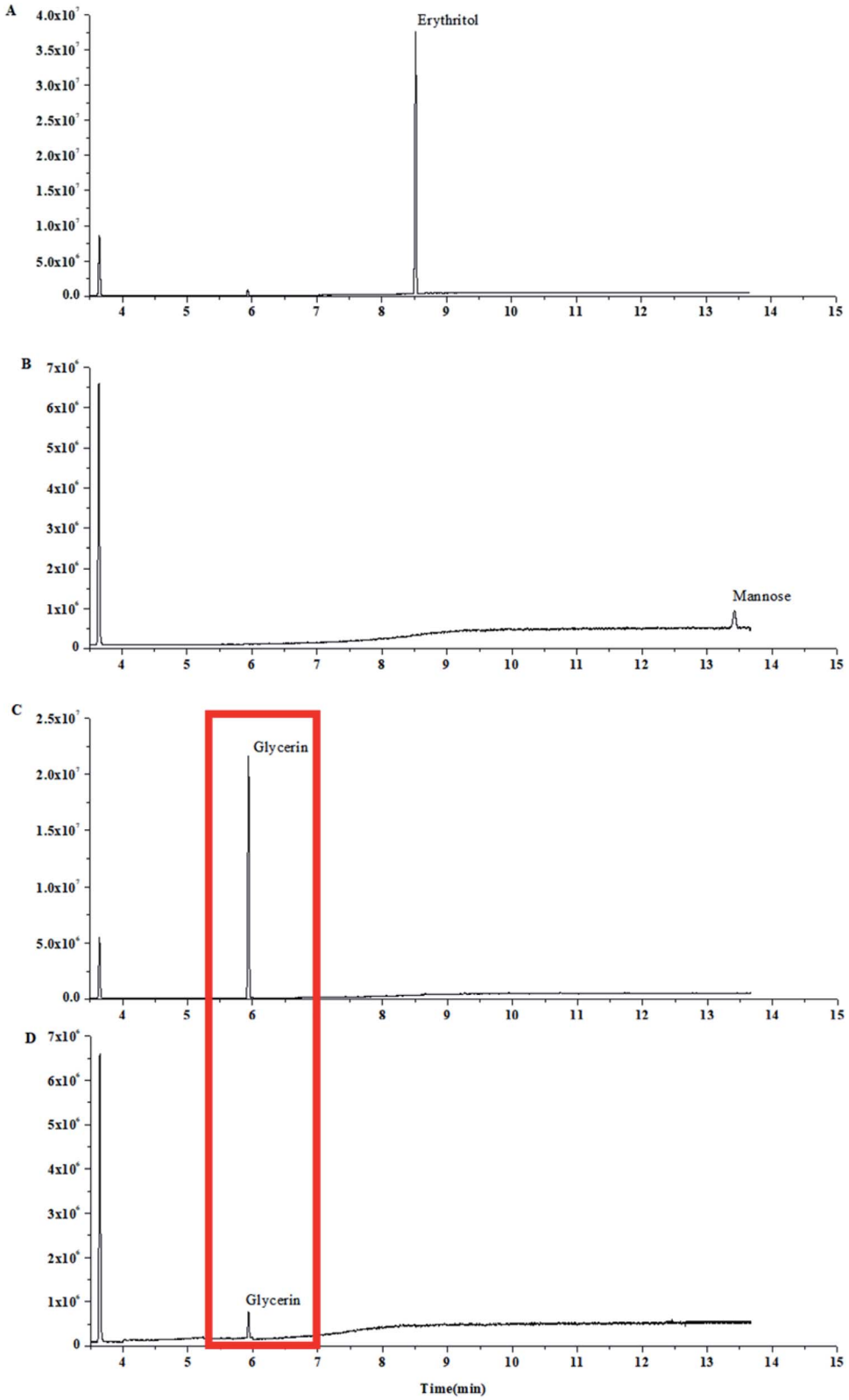

Fig. 4 Gas chromatography of erythritol (A), mannose (B), glycerin (C) and LVP (D) after Smith degradation.

Table 1 Methylation analyses of reduced LVP

Retention time (min)	Methylated sugar	Linkage[b]	Molar percentage (%)	Main MS (*m*/*z*)
11.473	2,3,4,6-Me_4-Man*p*	T	44.1	43, 57, 73, 85, 101, 117, 129, 145, 161, 205
12.449	2,3,6-Me_3-Man[a]	→4) Man (1→	42.9	43, 71, 87, 99, 117, 129, 161, 189
13.318	2,3-Me_2-Man	→4,6) Man (1→	13	43, 71, 87, 99, 129, 189, 233

[a] Me, methyl; Man, mannose. [b] In the linkage column, the combination of numbers and arrows represents glycosidic linkages, and the middle words (Man, mannose) represent the corresponding monosaccharide units.

a homogeneity polysaccharide, and the molecular weight was calculated to be about 16.842 kDa on basis of the calibration curve of dextran standards. In addition, monosaccharide composition of LVP was examined by HPLC. It is known that monosaccharide compositions of polysaccharide have effects on its biological activities. Only one peak (Fig. 2D) appeared in the LVP corresponding to mannose standard in accordance with retention time, showing the basic monosaccharide composition of LVP is mannan instead of other polysaccharides.

3.3 Chemical characteristics of LVP

No absorbance at 280 nm by ultraviolet spectra analysis was measured (Fig. 3A), which showed the LVP comprised no or little proteins, with high purity. The infrared spectrometry of LVP was presented in Fig. 3B. The stretching intense characteristic peaks at 3478.94 cm^{-1} indicated the polysaccharide chains with hydroxyl stretching. The band at 1654.48 cm^{-1} represented the absorption peak of bound water in LVP. The peak around 1086.03 cm^{-1} revealed that pyranose rings forms the skeletal modes of LVP, which was consistent with the results.[5] The microstructures of LVP were characterized by SEM (Fig. 3C). LVP showed the same folds as the brain and those ovoid-shaped particles were distributed throughout its microstructure at random, while the polysaccharides in other studies were shown to be flaky and tubular,[20] which may be related to the aggregation of polysaccharides, leading to various microstructures. There were some large voids in the honeycomb-like structure of the polysaccharide. The possible reason was that the molecular weight of LVP is relatively low. The loose structure of the polysaccharide allowed it to interact with other substances, indicating that it can participate in more multiplex biological activities.[6]

3.4 Periodate oxidation–Smith degradation analysis

After 84 h of periodate oxidation experiment, the absorbance of oxidation product at 223 nm was steady. The reaction consumes 1.8328 mmol $NaIO_4$ and little formic acid was produced. Combined with the Smith degradation result shown in Fig. 4, the Smith degradation products only contain erythritol (Fig. 4C and D), indicating that the polysaccharide chain structure of LVP partly consisted of (1→4)-linked and (1→4,6)-linked glycosidic bonds.[21] Periodate oxidation and Smith degradation can predict glycosidic linkages of the polysaccharide. At the same time, methylation analysis and NMR spectroscopy were performed to further determine the glycosidic bonds of monosaccharides in LVP.

3.5 Methylation and NMR analysis of LVP

Methylation analysis was used to identify the type of linkage between glycosyl residues. For LVP, the three peak signals were identified on the total ion chromatogram using the combined

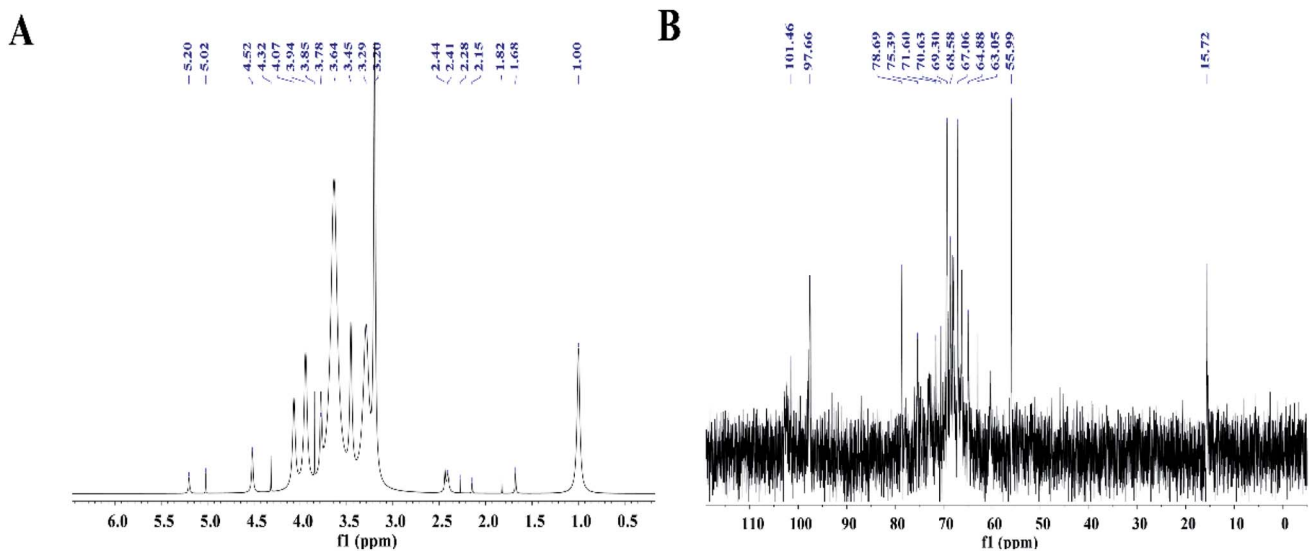

Fig. 5 NMR spectra of LVP and its predicted structure in D_2O. (A) ^1H NMR spectrum; (B) ^{13}C NMR spectrum.

information of diagnostic fragments and monosaccharide composition analysis. The results were showed in Table 1. According to the results of GC-MS analysis, three partially methylated sugar alcohol acetates, namely 2,3,4,6-Me_4-Man*p*, 2,3,6-Me_3-Man and 2,3-Me_3-Man in the molar percentage of 44.1%, 42.9% and 13% were identified, respectively (Table 1). The molar ratio of 2,3,6-Me_3-Man*p* (1,4-linked Man, Me, methyl; Man, mannose) was higher than that of 2,3-Me_2-Man*p* (1,4,6-linked Man), revealed that the main chain included the →4) Man*p* (1→ residues. The degree of branch (DB) was calculated as follows:[21] DB = (NT + NB)/(NT + NB + NL), where NT, NB, and NL are the numbers of terminal, branch, and linear residues, respectively. The calculated DB of LVP was 0.571 on basis of methylation data, showing its highly branched characteristic.

The structure of LVP was further verified by NMR spectra and the signals of LVP in the ^{1}H and ^{13}C NMR spectra were showed in Fig. 5A (^{1}H NMR spectra) and Fig. 5B (^{13}C NMR spectra). All the peaks of the ^{1}H NMR spectra appeared between δ 1 and 6 ppm, which was typical of the NMR spectra of polysaccharides. There were no resonances observed between δ 6 and 8 ppm, revealed that LVP did not include phenolic or ferulic acid components. The proton signals of LVP in the hydrogen spectrum were focused on the range of δ 3.20 to 5.20 ppm, besides, the proton signal also appeared sporadically at δ 1.00 ppm. Among them, the chemical shifts of most protons were in the range of δ 3–4 ppm because of the shielding effect of hydroxyl groups, and serious overlap between signals caused difficulty in analysis. Moreover, two anomeric protons at δ 5.20 and 5.02 ppm, which were characterized as →4-α-Man*p*-(1→ and →4,6-α-Man*p*-(1→, respectively. As shown in Fig. 5B, the anomeric carbon signals of LVP in the carbon spectrum were focused on the range of δ 55.99 to 78.69 ppm, besides, the carbon signal also appeared sporadically at δ 15.72 ppm. Generally, the anomeric carbon signals were mostly in the range of δ 95–110 ppm, where the signals at δ 101.46 and 97.66 ppm suggested the presence of (1→4)-α-Man and (1→4,6)-α-Man. In the final analysis, the NMR results and the methylation analysis results were basically consistent.

Based on FTIR, methylation and GC-MS analysis, and NMR, the isolated LVP was characterized to be mannan, and the linkages in the mannan were found to comprise Man*p*, (1→4)-α-Man and (1→4,6)-α-Man. →4-α-Man*p*-(1→ is likely as a branching unit in the main chain, while →4,6-α-Man*p*-(1→ may be located in both main chain and side chain. The more detailed information about the locations and sequences of the two glycosidic linkages (T; 1,4-; 1,4,6-) will be clarified in the future.

3.6 Effect of LVP on organ indices in CP-treated mice

The organ index may be used to reflect organ function of an organism. Spleen, thymus, and liver are the significant immune organs, which involved in the humoral and cellular immunity.[22] Table 2 showed that compared with the CK group, the spleen, thymus and liver indices of the CP groups (CP^- and CP^+) decreased, showing that the mice immunosuppression model was successfully established. Administration of LVP obviously increased the organ indices of mice when compared to those of the

Table 2 Effects of LVP on organ indices, lymphocytes proliferation, phagocytosis of macrophages and serum half hemolysis levels (HC_{50})[a]

Group	Dose (mg kg^{-1} bw^{-1})	Body weight (g)	Spleen index	Thymus index	Liver index	DTH/mm	WBC/(10^9 L^{-1})	LYM/(10^9 L^{-1})	Macrophage phagocytosis (A_{540} nm)	HC_{50}
CK	NO	27.27 ± 0.97	8.52 ± 0.89^{bc}	2.15 ± 0.18^{bc}	54.14 ± 2.30^{bc}	0.64 ± 0.11^{bc}	5.25 ± 0.51^{bc}	3.15 ± 0.50^{bc}	0.1763 ± 0.0091^{b}	259.51 ± 16.85^{bc}
CP^-	NO	25.68 ± 0.84	7.60 ± 1.110^{a}	1.35 ± 0.14^{a}	50.69 ± 2.10^{a}	1.41 ± 0.24^{ac}	4.10 ± 0.58^{ac}	2.11 ± 0.38^{a}	0.1944 ± 0.015^{ac}	140.73 ± 2.34^{a}
CP^+	400	25.75 ± 0.97	7.87 ± 0.67^{a}	1.46 ± 0.22^{a}	50.99 ± 3.10^{a}	1.79 ± 0.18^{ab}	5.08 ± 0.97^{ab}	2.47 ± 0.44^{a}	0.1722 ± 0.029^{b}	148.98 ± 14.01^{a}
LP	200	26.68 ± 0.91^{bc}	5.54 ± 0.81^{abc}	1.17 ± 0.25^{abc}	48.11 ± 1.80^{abc}	1.08 ± 0.14^{ac}	6.98 ± 2.00^{abc}	3.88 ± 0.72^{bc}	0.1632 ± 0.010^{b}	269.18 ± 17.86^{bc}
MP	400	27.53 ± 0.78^{bc}	5.88 ± 1.10^{abc}	1.19 ± 0.19^{abc}	49.73 ± 1.00^{abc}	1.14 ± 0.13^{ac}	5.13 ± 0.88^{bc}	2.98 ± 0.54^{bc}	0.1616 ± 0.022^{b}	262.82 ± 19.61^{bc}
HP	800	28.79 ± 0.87^{bc}	6.04 ± 1.20^{abc}	1.27 ± 0.12^{abc}	48.35 ± 1.60^{abc}	1.18 ± 0.11^{ac}	4.72 ± 1.00^{abc}	2.69 ± 0.55	0.1598 ± 0.015^{b}	260.93 ± 25.27^{bc}

[a] CK: control group; CP^-: negative model control group; CP^+: positive model control group; LP, MP, and HP: polysaccharide group, normal diet with LVP at the dose of 200, 400, and 800 mg kg^{-1} bw^{-1}. The data are presented as means ± SD (n = 12). [a]Compared to the CK group ($p < 0.05$); [b]Compared to the CP^- group ($p < 0.05$); [c]Compared to the CP^- group ($p < 0.05$).

CP groups ($p < 0.05$), and worked in a dose-dependent manner, which closely resembled to polysaccharides from *Ganoderma atrum*.[23] These suggested that LVP showed mucosal immune regulation. Furthermore, compared with the CP^- group, LVP administration statistically increased the spleen, thymus and liver indices in the model-group mice. These results revealed that LVP could enhance the weight of the immune organ and have protective effects against CP^- induced immunosuppression in mice.

3.7 Effect of LVP on delayed hypersensitivity in immunosuppressed mice

DTH is a hypersensitive cytoimmunity mediated by T lymphocytes. Delayed-type hypersensitivity (DTH) is a CCR7 effect memory T lymphocyte infiltrating the inflammatory response mediated by the injection site of the antigen whose immune system has germinated. The SRBCs can be integrated with abdominal wall skin proteins into complete antigens, therefore irritating the proliferation of T-lymphocytes into sensitized lymphocytes. DTH responses to SRBCs in infected mice were measured at 24 h after secondary sensitization of SRBC in Table 2. Compared with the CK group, the mean of DTH responses radically increased in immunosuppressed mice ($p < 0.05$), but was obviously weaken compared with the model group ($p < 0.05$). There were no obvious differences between the mean of DTH responses of these three LVP groups (LP, MP, and HP groups), but the means were significantly lower than those of CP^- group and CP^+ group ($p < 0.05$). Results showed LVP could improve immune function of mice by decreasing the mean of DTH responses.

3.8 Effect of LVP on MPS function by carbon clearance test in immunosuppressed mice

The effects of LVP on macrophage activation were determined in carbon clearance tests, the inert carbon particles injected into the vein can be easily removed from the blood by macrophages.[24] The

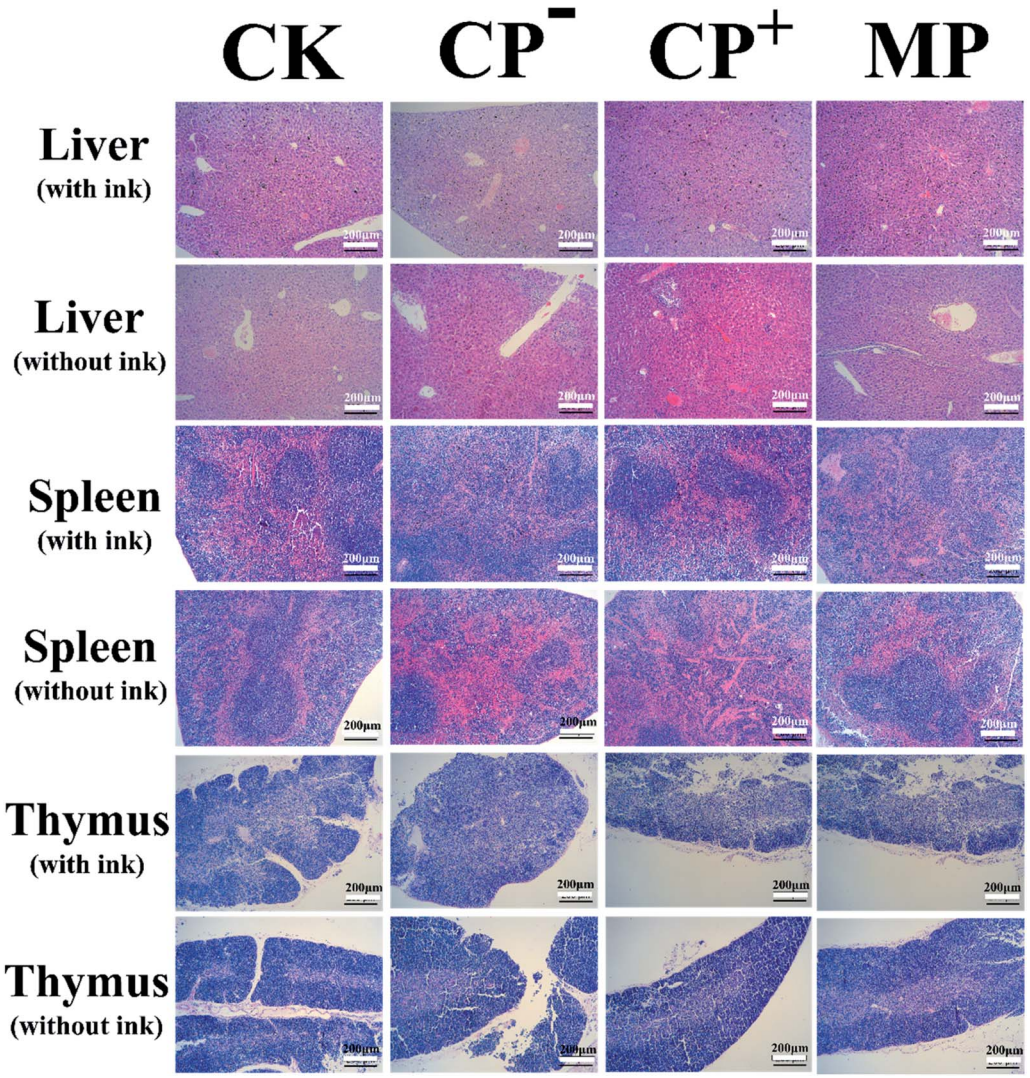

Fig. 6 Gross morphological changes in the livers, spleens and thymuses of mice. The mice were euthanized after a feeding period of 40 days. The livers, spleens and thymuses were removed immediately, and the gross morphology and surface color were observed. CK: control group; CP^-: negative model control group; CP^+: positive model control group; MP: LVP-treated group, normal diet with LVP at the dose of 400 mg kg^{-1} bw^{-1}.

phagocytic function of macrophages is one of the main indicators reflecting the non-specific immune function of animals.[24] The phagocytic activity of macrophages decreased in the CP-treated groups when compared with that of normal group (Table 2). However, compared with CP^- group, the phagocytic activity of the LVP-treated groups was significantly increased ($p < 0.05$) in a dose-dependent fashion. LVP treatment also obviously increased phagocytic activity in comparison with the CK group ($p < 0.05$). It was clarified LVP could effectively improve the phagocytic effect of macrophages in immunosuppressed mice.

3.9 Effects of LVP on serum half hemolysis levels (HC_{50}) in immunosuppressed mice

The formation of serum hemolysis immunized with SRBC shows the humoral immunologic capability.[25] Table 2 showed that HC_{50} (140.73 and 148.98) in CP^- and CP^+ groups were significantly lower than those in CK, LP, MP and HP (259.51, 269.18, 262.82 and 260.93) ($p < 0.05$). Additionally, the HC_{50} in CP^+ group was obviously higher than that in CP^- group ($p < 0.05$), which may be associated with the immune repair function of polysaccharides. Therefore, LVP may be have a suppressive activity on the humoral immunity.

3.10 Effects of LVP on lymphocytes proliferation in immunosuppressed mice

The inflammation of mice, and the anti-inflammatory levels and immune function level can be evaluated by the white blood cells (WBC) and the number of lymphocyte immune cells (LYM). Table 2 showed that the WBC of CP^- group (4.10×10^9 L^{-1}) obviously reduced compared with the LVP treatment groups and the CK group. The WBC in CP^+ group (5.08×10^9 L^{-1}) was obviously higher than that in CP^- group ($p < 0.05$), which may be associated with the immune repair function of polysaccharide. The LYM in CK group (3.15×10^9 L^{-1}) was significantly higher than that in other groups ($p < 0.05$), which may be related to the individual differences in mice and the involvement of polysaccharide in immune regulation reaction.

3.11 Morphological changes of the liver, spleen and thymus

The morphological changes in the liver, spleen and thymus were measured to assess the effects of LVP on these immune organs in Fig. 6. Liver macrophages, also known as Kupffer cells, are involved in immunomodulation and hepatocyte vacuolation can be characterized by inflammation to characterize the degree of hepatocellular injury. Hematoxylin–eosin (HE) staining showed that MP group (1–5%) decreased the proportion of vacuolation of the Kupffer cells (Fig. 6), compared with CP-treated group (5–10%, CP^- group; 10–20%, CP^+ group). Compared with the mice injected with ink, no liver abnormalities were observed in mice in the MP group. However, the appearance of CP^- group and CP^+ group without ink were worse than that of mice injected with ink. The spleen sections of mice injected with ink (Fig. 6) illustrated that the MP group facilitated splenocyte proliferation and decreased pigment deposits compared with the CP-treated group. The spleen sections of mice injected without ink (Fig. 6) showed the connective tissue of the membrane protruded into the spleen resulting in large amounts of hemolysis in CP^- group. The CP^+ group was observed with many trabeculae and spleen bodies. The distribution of medulla, trabecular and spleen bodies in the MP group and CK group were no abnormalities. The thymus sections of mice injected with ink (Fig. 6) showed that the ratio of the outer and inner layers of the thymus pathological of the CP^- and CP^+ groups were significantly decreased, which were lower than that of the CK group. The results without ink were similar to those of the thymus of mice injected with ink. The proportion of not removing carbon from the thymus in the MP group was less than that in the CP^+ group and CK group. These results suggested that LVP protected the immune organs against CP-induced impairment.

Combining the above results, we speculated that LVP may express its systemic immunomodulating effects by stimulating the intestinal mucosal immunity, which was similar to polysaccharides from *Citrus unshiu*.[23] However, the deeper understanding of mechanisms of immunomodulatory activity by intraperitoneal administration of LVP should be further studied.

4. Conclusion

In summary, a neutral polysaccharide LVP was isolated from *Lactarius volemus* Fr. planted in a pine forest in Yunnan, China. The isolated LVP was characterized to be mannan, and the linkages in the mannan were found to comprise Man*p*, (1→4)-α-Man and (1→4,6)-α-Man. The preliminary activity test revealed that LVP significantly improved the immune cell proliferation and serum half hemolysis levels, enhanced the immune response and stimulated phagocytosis. These results may further provide theoretical foundation for the extensive use of LVP in functional food and pharmaceutical industries. Other studies are currently underway to prepare large amounts of LVP and investigate its molecular mechanism of *in vivo* immunostimulatory effects including Ca^{2+}, cAMP, cGMP, NO, and other cellular signals in CP-induced immunosuppressed mice. Additional studies such as *in vitro* cell experiments will be conducted to obtain cell signals to explore the types of polysaccharide receptors and immune mechanisms.

Conflicts of interest

There are no conflicts to declare.

Acknowledgements

This study was supported by the National Natural Science Foundation of China (No. 31771908), and the Guangdong Science and Technology Program key project (201903010015).

References

1 Y. Shi, Q. X. Chen, Q. Wang, K. K. Song and L. Qiu, Inhibitory effects of cinnamic acid and its derivatives on the diphenolase activity of mushroom (*Agaricus bisporus*) tyrosinase, *Food Chem.*, 2005, **92**, 707–712.

2 F. Wu, C. Zhou, D. Zhou, S. Ou, X. Zhang and H. Huang, Structure characterization of a novel polysaccharide from *Hericium erinaceus* fruiting bodies and its immunomodulatory activities, *Food Funct.*, 2018, **9**, 294–306.
3 D. Morales, R. Rutckeviski, M. Villalva, H. Abreu, C. Solerrivas, S. Santoyo, I. Marcello and F. R. Smiderle, Isolation and comparison of α- and β-D-glucans from shiitake mushrooms (*Lentinula edodes*) with different biological activities, *Carbohydr. Polym.*, 2020, 115521.
4 K. Kobata, T. Wada, Y. Hayashi and H. Shibata, Volemolide, a novel norsterol from the fungus *Lactarius volemus*, *Biosci., Biotechnol., Biochem.*, 1994, **58**, 1542–1544.
5 M. Ozyurek, M. Bener, K. Guclu and R. Apak, Antioxidant/antiradical properties of microwave-assisted extracts of three wild edible mushrooms, *Food Chem.*, 2014, **157**, 323–331.
6 D. Zhou, P. Li, Z. Dong, T. Wang, K. Sun, Y. Zhao, B. Wang and Y. Chen, Structure and immunoregulatory activity of β-d-galactofuranose-containing polysaccharides from the medicinal fungus *Shiraia bambusicola*, *Int. J. Biol. Macromol.*, 2019, **129**, 530–537.
7 H. G. Liu, J. Zhang, T. Li, Y. D. Shi and Y. Z. Wang, Mineral Element Levels in Wild Edible Mushrooms from Yunnan, China, *Biol. Trace Elem. Res.*, 2012, **147**, 341–345.
8 J. M. Yue, S. N. Chen, Z. W. Lin and H. D. Sun, Sterols from the fungus *Lactarium volemus*, *Phytochemistry*, 2001, **56**, 801–806, DOI: 10.1016/S0031-9422(00)00490-8.
9 M. J. Alves, I. C. Ferreira, H. J. Froufe, R. M. V. Abreu, A. Martins and M. Pintado, Antimicrobial activity of phenolic compounds identified in wild mushrooms, SAR analysis and docking studies, *J. Appl. Microbiol.*, 2013, **115**, 346–357.
10 M. Ahlmann and G. Hempel, The effect of cyclophosphamide on the immune system: implications for clinical cancer therapy, *Cancer Chemother. Pharmacol.*, 2016, **78**, 661–671.
11 Q. Yu, S. P. Nie, J. Q. Wang, D. F. Huang, W. J. Li and M. Y. Xie, Molecular mechanism underlying chemoprotective effects of *Ganoderma atrum* polysaccharide in cyclophosphamide-induced immunosuppressed mice, *J. Funct. Foods*, 2015, **15**, 52–60.
12 Q. Xiang, Q. Yu, H. Wang, M. Zhao, S. Liu, S. Nie and M. Xie, Immunomodulatory effect of *Ganoderma atrum* polysaccharides on Th17/Treg balance, *J. Funct. Foods*, 2018, **45**, 215–222.
13 P. Düwell, S. Heidegger and S. Kobold, Innate immune stimulation in cancer therapy, *Hematol. Oncol. Clin. N. Am.*, 2019, **33**, 215–231.
14 J. Xie, L. Zou, X. Luo, L. Qiu, Q. Wei, D. Luo, Y. Wu and Y. Jiao, Structural characterization and immunomodulating activities of a novel polysaccharide from *Nervilia fordii*, *Int. J. Biol. Macromol.*, 2018, **114**, 520–528.
15 W. Liao, Z. Luo, D. Liu, Z. Ning, J. Yang and J. Ren, Structure characterization of a novel polysaccharide from *Dictyophora indusiata* and its macrophage immunomodulatory activities, *J. Agric. Food Chem.*, 2015, **63**, 535–544.
16 Y. Huang, S. Zhao, K. Yao, D. Liu, X. Peng, J. Huang, Y. Huang and L. Li, Physicochemical, microbiological, rheological, and sensory properties of yoghurts with new polysaccharide extracts from *Lactarius volemus* Fr. using three probiotics, *Int. J. Dairy Technol.*, 2020, **73**, 168–181.
17 A. Villares, Polysaccharides from the edible mushroom *Calocybe gambosa*: structure and chain conformation of a (1→4), (1→6)-linked glucan, *Carbohydr. Res.*, 2013, **375**, 153–157.
18 I. Ciucanu and F. Kerek, A simple and rapid method for the permethylation of carbohydrates, *Carbohydr. Res.*, 1984, **131**, 209–217.
19 J. Liao and H. Huang, Magnetic chitin hydrogels prepared from Hericium erinaceus residues with tunable characteristics: a novel biosorbent for Cu^{2+} removal, *Carbohydr. Polym.*, 2019, **220**, 191–201.
20 Y. Zhu, C. Wang, S. Jia, B. Wang, K. Zhou, S. Chen, Y. Yang and S. Liu, Purification, characterization and antioxidant activity of the exopolysaccharide from *Weissella cibaria* SJ14 isolated from Sichuan paocai, *Int. J. Biol. Macromol.*, 2018, **115**, 820–828.
21 X. Zhang, X. Kong, Y. Hao, X. Zhang and Z. Zhu, Chemical structure and inhibition on α-glucosidase of polysaccharide with alkaline-extracted from *glycyrrhiza* inflata residue, *Int. J. Biol. Macromol.*, 2020, **147**, 1125–1135.
22 M. Hamad, M. Whetsell and J. R. Klein, T cell precursors in the spleen give rise to complex t cell repertoires in the thymus and the intestine, *J. Immunol.*, 1995, **155**, 2866–2876.
23 S. Zhang, S. Nie, D. Huang, W. Li and M. Xie, Immunomodulatory effect of Ganoderma atrum polysaccharide on ct26 tumor-bearing mice, *Food Chem.*, 2013, **136**, 1213–1219.
24 G. H. Wu, C. L. Lu, J. G. Jiang, Z. Y. Li and Z. L. Huang, Regulation effect of polysaccharides from *pleurotus tuber-regium* (fr.) on the immune activity of mice macrophages, *Food Funct.*, 2014, **5**, 337–344.
25 D. L. Lodmell, R. K. Bergman and W. J. Hadlow, Antibody-forming cells and serum hemolysin responses of pastel and sapphire mink inoculated with aleutian disease virus, *Infect. Immun.*, 1973, **8**, 769–774.
26 T. K. Shackelford, G. J. LeBlanc, V. A. Weekes-Shackelford, A. L. Bleske-Rechek, H. A. Euler and S. Hoier, Psychological adaptation to human sperm competition, *Evol. Hum. Behav.*, 2002, **23**, 123–138.
27 X. Duan, S. Gao, J. Li, L. Wu, Y. Zhang and W. Li, Acute arsenic exposure induces inflammatory responses and CD4 + T cell subpopulations differentiation in spleen and thymus with the involvement of MAPK, NF-kB, and Nrf2, *Mol. Immunol.*, 2017, **81**, 160–172.

